RASĀYAN *J. Chem.*
Vol. 17 | No. 3 |1251-1257| July - September | 2024
ISSN: 0974-1496 | e-ISSN: 0976-0083 | CODEN: RJCABP
http://www.rasayanjournal.com
http://www.rasayanjournal.co.in

THE ROLE OF MgO ON THE OPTICAL CHARACTERISTICS AND STRUCTURAL PROPERTIES OF ANTIMONY-CALCIUM-BORATE GLASSES FOR OPTOELECTRONIC APPLICATIONS

A.Rajesh[1], Pallati Naresh[2], Jagram Anterbedy[1], K. Santosh Kumar[3] and Gangadhar Thalari[1],✉

[1]Department of Chemistry, Osmania University, Hyderabad-500007, Telangana, India
[2]Department of Physics, UCS Saifabad, Osmania University, Hyderabad-500004, Telangana, India
[3]Department of Chemistry, Geetanjali College of Engineering and Technology, Cheeryal Hyderabad-501301, Telangana, India
✉Corresponding Author: gangadharchemou@gmail.com

ABSTRACT

MgO-incorporated melt-derived glasses of compositions $xMgO\text{-}10CaO\text{-}10Sb_2O_3\text{-}(80\text{-}x)B_2O_3$ with molar ratios x=0,5,10,15,20mol% were synthesized. The basic amorphous structural confirmation was done using X-ray diffraction analysis of the glass series. Short range order and broad humps were presented in the spectra which is a characteristic nature of glassy amorphous solids. The increasing trends of density were found as a function of MgO content. The UV-Absorption spectral analysis on the glass samples revealed that the cut-off wavelength values were enhanced from 296nm to 363nm with additive MgO content. The Urbach energy values increased, whereas, indirect band gaps decreased with the entry of modifier MgO molar fraction. The higher refractive index 2.3 of the present glasses proved the suitability for optoelectronic device applications. The FT-IR spectra revealed the existence of various structural variations with the incorporation of MgO and showed the creation of NBOs.

Keywords: Refractive Index, Indirect Band Gap, Molar Volume, Urbach Edge, Molar Volume, NBOs

RASĀYAN *J. Chem.*, Vol. 17, No.3, 2024

INTRODUCTION

Oxide glasses are widely used for many applications over the other types of glasses. Borate and silicate oxide glasses are the special glasses exhibiting their efficacy in the current needs of industry and biomedical applications.[1-2] Most of the bio-glasses (BGs) are the components of borate and silicate-based matrix. Due to the consistency of the trigonal and tetrahedral BO_3 and BO_4 units in the borate-based glasses and also due to the transparency, brittleness, rigidity, and chemical durability, these are the prominent and suitable candidates for the optoelectronic device, battery, and tissue engineering applications. The metal oxide-incorporated borate glasses stood in the front line in terms of the enhanced properties in dental treatments and bone regeneration applications. In particular, MgO, Ag_2O, ZnO & CaO-incorporated glassy matrices proved their efficiency for biomedical applications with enhanced zones of inhibitions. In recent days, the borate glasses glassy matrices have also been used in radiation shielding applications due to higher densities when it is doped with heavy metal oxides.[3-5] Antimony oxide acts like a network modifier in the glass network. It is familiar for its higher density, higher refractive index, and third-order non-linear optical susceptibility. Due to these qualities, Sb2O3-containing borate glasses show their efficiency in the fabrication of optoelectronic device applications, fiber-optics communication systems, and bio-active related applications. Sb^{+3} ions influence the glass network and destroy it, in different ways in the formation of creations of non-bridging oxygens. The role of MgO in the glass network is as a network modifier. The MgO incorporation into the borate glass network results in the improvement of biological activity and mechanical properties, and also chemical durability of the glass networks. Mg^{+2} is a trace component of the human body and also human bone.[6] Due to the high melting points and thermal stability of MgO, it exhibits an excellent spectrum of applications in various fields. CaO-MgO-containing glass-ceramics widely used in industry applications,

http://doi.org/10.31788/RJC.2024.1738863

low thermal expansion, super mechanical applications, dental-related applications, fractures-related applications, etc.[7] The presence of CaO causes the enhancement of antimicrobial efficiency in the form of Ca^{+2} ions in the glass network. These ions kill the cells and DNA of the bacterial strains.[8] The present work focused on the role of MgO in the structural variations of borate glass network with its molar contents, the optical characteristics dependency on the MgO content, the effect of MgO on the density-based physical parameters with consuming boric acid and occupancy with dopant MgO. It also deals with the structure-composition ratio and its effect on various properties of the glass compositions of the present study.

EXPERIMENTAL

Material and Methods

The melt-quenching method was adopted for the preparations of the glass compositions as increasing content of MgO and decreasing content of B_2O_3, whereas, CaO and Sb_2O_3 remain fixed in the glass composition. The formula of chemical compositions in the stoichiometric ratios selected as xMgO-10CaO-10Sb_2O_3-(80-x)B_2O_3 with molar ratios x=0,5,10,15,20mol%. The oxide compositions were mixed in a porcelain crucible and kept in a furnace maintained at 1205°C. After 30 minutes, the powder mixture was melted and the molten liquid was stirred thoroughly to get uniform mixing. Further, it was poured on a metal plate and rapidly quenched with a presser. The required glassy samples were formed, and, annealed to remove the strains at 300^0C for 12 hours. The X-ray diffraction studies were done on a Philips XPert'Pro diffractometer at room temperature in the Braggs angle ranging from 10-80°. The density measurements were done using Dona digital balance. The optical characteristics were studied in the wavelength ranges from 200nm-1000nm. The FT-IR measurements were done using the KBr pellet method in the wavenumber range 400-4000cm^{-1}.

RESULTS AND DISCUSSION

XRD Studies

The X-ray diffraction spectrograms of the MgO-incorporated calcium-antimony borate glasses are depicted in the Fig.-1. In the spectra, only a broad hump was appeared in the spectra near 28° and also found in short-range order. The broad humps with lower intensity were found. Even, with the addition of the glass network modifier also no changes were found in the spectra. The results of XRD reveal the strong amorphous behavior of the glasses selected for the investigation.[9]

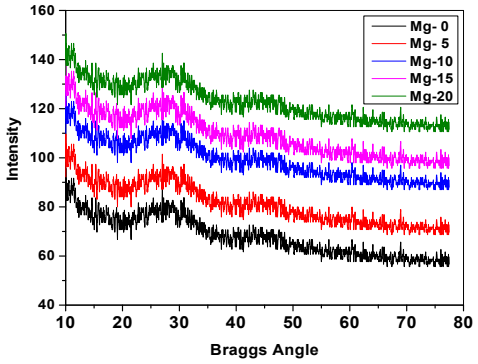

Fig.-1: The XRD Spectra of BSCM Glassy Series

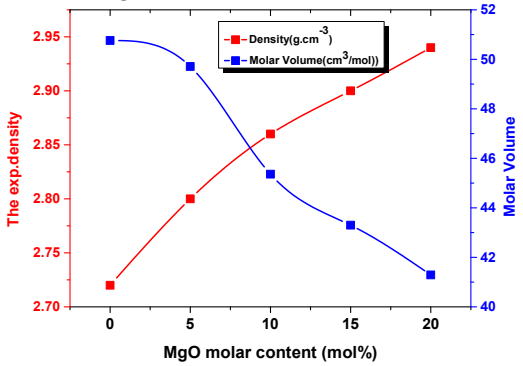

Fig.-2: The Variation of Density and Molar Volume with MgO

Archimedes Method: Density and its Dependent Physical Properties

Archimedes' approach generated the experimental density results as follows. As given in Table-1 the density of the glass system is increased from 2.72 $g.cm^{-3}$ to 2.94 $g.cm^{-3}$ by the addition of MgO. This linear increase in density concerning the addition of the MgO may be due to the higher molecular weight of MgO (3.58 $g.cm^{-3}$) in comparison to that of B_2O_3 (3.11 $g.cm^{-3}$).[10] Molar volume of the MgO dopant glass system is changed from 50.76 cm^3/mol to 41.29 cm^3/mol and continuously decreases with the addition of the dopant. This decreased trend showed the reciprocal relationship with the density evaluated by Archimedes method as shown in Fig.-2. It is also observed that the O.P.D. of the evaluated glass system has also shown an increase in its value from 55.15 to 58.11 g.atm/l units with the increase in the

amount of MgO. This increase in O.P.D. may be attributed to the increased number of Non-Bridging Oxygens which may cause significant changes in the physical parameters of the glass system. The measured and evaluated values of the physical properties by Archimedes method and derived quantities are given in Table-1.

Optical Studies

The absorption mode of optical spectra of MgO incorporated glass series is shown in Fig.-3. It was observed that the cutoff wavelength (λ_c) increased from 296 nm to 363 nm with the addition of MgO content. The increase in wavelength of cut-off may be attributed to the formation of NBOs with the increasing concentration of MgO.[11]

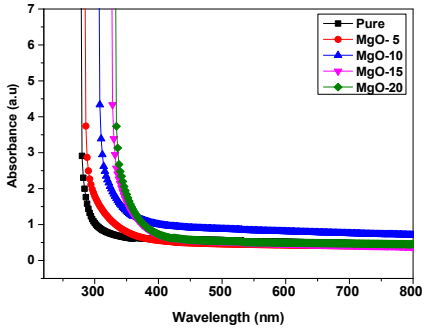

Fig.-3: The UV-Spectra of MgO Glass Series

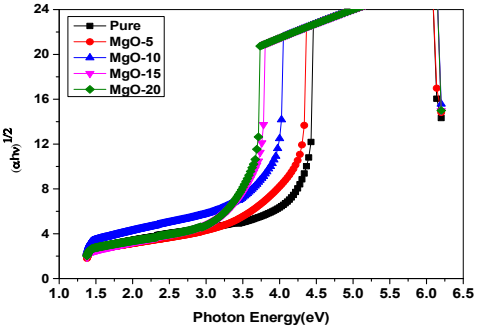

Fig.-4: The Tauc Plots of Indirect Band Gap

The highest cut-off wavelength λ_c value was observed at 20 mol% of the MgO in the glass system. The formation of BO_3 units from BO_4 units occurs as the concentration of MgO rises, increasing the refractive index and decreasing band gap energies. As the molar content of MgO increased, the E_{opt} (indirect) values dropped from 4.04 eV to 3.07 eV, as shown in Fig.-4. Table-1 illustrates how the addition of MgO percentage affected the direct energy band gap of the current glasses, which varied between 4.32 eV and 3.60 eV. As shown in Table, the direct band gap of the glasses under study varied with altering MgO content, ranging from 4.32 eV to 3.60 eV. Higher refractive index values and a lower band gap energy will follow from this. Notable changes are happening as the concentration of Mg^{2+} ions grows.[12] The least-square fit of the plots' straight lines was used to compute the Urbach energies ΔE as shown in Fig.-6. The ΔE was found to be growing and shifted from 0.65 eV to 0.85 eV. In other words, the presence of NBOs causes the glass network structure to become increasingly random as MgO is added. As the concentration of the network modifiers increases, structural alterations in the host glass are probably the origin of this development. The least-square fit of the plots' straight lines was used to compute the Urbach energies ΔE as shown in Fig.-6.

Table-1: Physical & Optical Parameters of MgO Series

Parameter	Sample Code				
	MgO-0	MgO-5	MgO-10	MgO-15	MgO-20
Density ($g.cm^{-3}$)	2.72	2.80	2.86	2.90	2.94
Molar mass ($g.mol^{-1}$)	138.09	133.92	129.75	125.58	121.41
Molar volume (cm^3mol^{-1}) (±0.1)	50.76	49.71	45.36	43.30	41.29
OPD ($g.atm.1^{-1}$) (±0.15)	55.15	56.45	57.31	57.73	58.11
Cut off wavelength (nm) (±1nm)	296	312	324	361	363
Indirect energy band gap (±0.01eV)	3.90	3.76	3.54	3.41	3.37
Direct energy band gap(±0.01eV)	3.97	4.21	3.85	3.68	3.60
Urbach edge (±0.01eV)	0.65	0.72	0.76	0.80	0.85
Index of Refraction	2.12	2.14	2.19	2.22	2.28
Dielectric constant	4.49	4.62	4.79	4.92	5.29
Reflection loss	0.537	0.546	0.558	0.566	0.588
Molar refraction (cm^3/mol)	25.14	24.53	23.66	22.57	22.31
Electronic polarizability ($10^{-24}cm^{-3}$)	7.25	7.36	7.42	7.48	7.86

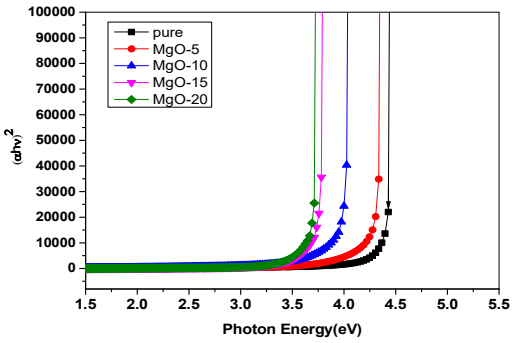

Fig.-5: Tauc's Plots of Direct Band Gap

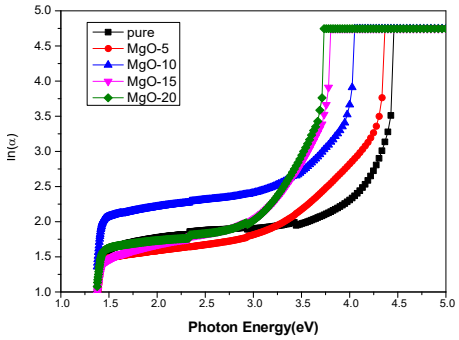

Fig.-6: The Urbach Plots of MgO Glass Series

The ΔE was found to be growing and shifted from 0.65 eV to 0.85 eV. In other words, the presence of NBOs causes the glass network structure to become increasingly random as MgO is added. As the concentration of the network modifiers increases, structural alterations in the host glass are probably the origin of this developing disorder in the glass system.[13-15]

With each rise of MgO, an increasing trend for the refractive index and a decreasing trend for molar refraction were observed. The presence of Sb2O3 and an increase in the MgO concentration could be the cause of the higher refractive index values (2.12-2.32). By adding MgO, the electronic polarizability changed and was discovered to be in the range of 10^{-24}. When MgO was added to the glass network, the molar refraction fluctuated between 25.14 cm^3/mol to 22.31 cm^3/mol and the reflection loss increased, Fig.-7 shows changes in the energy of the relative refractive index and the indirect band gap as a function of MgO.

FT-IR Spectra of BSC-Mg- Series

Glass sample series BSC-Mg The 400–4000 cm^{-1} wavenumber range was used to record FTIR spectra. For glass samples in particular, FTIR spectroscopy is a useful and practical method for determining the structure and functional groups of molecules. Figure-8 (a-e) shows the FTIR spectra of the BSC-Mg glass series, where the percentage of Mg-O content is increasing and the percentage of B_2O_3 content is decreasing. Peak assignments for the associated stretching frequency of the BSC-Mg series are provided in Table-2. Antimony and calcium have lower mass numbers than boron, which has a high mass number in this glass series.[16] There are four main stretching vibration peaks visible in the FTIR spectra. Among these vibration peaks, boron peaks appeared above 500 cm^{-1}, or in the mid-infrared range.[17-18] The following is the position of the boron stretching frequency vibrations. This region contained three sizable peaks: one at 1105 cm^{-1}, which might have been brought on by the BO bonds in BO_4 stretching vibrations, and another at 1270 cm^{-1}, which might have been brought on by the B-O bond vibrations in BO_3. B-O-B linkage vibrations were the cause of the large peak that was seen in this area.[19-20]

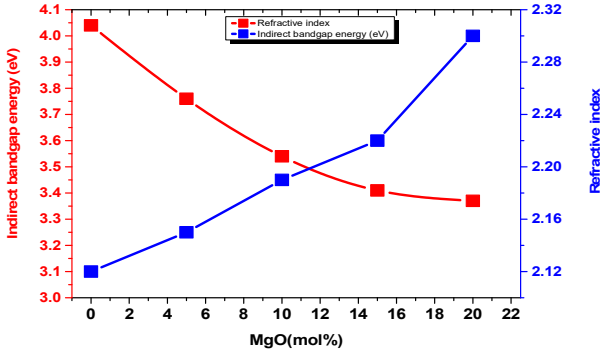

Fig.-7: The Variations in Refractive Index and Indirect Band Gap of MgO Incorporated Glass Series

The structure of the Ca-O-containing glass form is Ca_2O_3, and stretching vibration peaks were identified at the 910 cm^{-1} areas; these may be the result of Ca_2O_3 bending vibrations. The Mg-O bending vibrations that peak at 400 cm-1 are mostly caused by the Mg^{2+} ion, the lightest metal in this series of borate glasses

with a structure similar to Mg-O.[21-22] The peak positions of the FTIR spectra are presented in Table-2. Mg-O molar percentage increases from 0 to 20 in the current glass system, with variations of 5 moles in the boron antimony glass system. The FTIR band peak positions in the BSC-Mg glass series system were mostly observed at 395–418 cm^{-1}, 465-472 cm^{-1}, 492-512 cm^{-1}, 695-700 cm^{-1}, 793–812 cm^{-1}, 1219–1225 cm^{-1}, and 2900–2981 cm^{-1}. For Mg-O vibrations, the first peak's faint peak, which is between 395 and 418 cm^{-1}, corresponds to the Mg-O band. Two strong peaks developed, one at 465–472 cm^{-1} and 695-700 cm^{-1} which is related to the bending vibrations of B-O-B of BO_3 and Stretching vibrations of Sb-O-Sb in Sb-O linkage respectively, and another at 1219–1225 cm^{-1}, which is induced by the bending vibrations of the B–O–B bond in BO_4 units. Additionally, a large peak appeared, mostly around 1435-1445 cm^{-1}, which is connected to the oxygen ion of the BO_3 symmetric unit's bridge stretching vibration .[23-24]

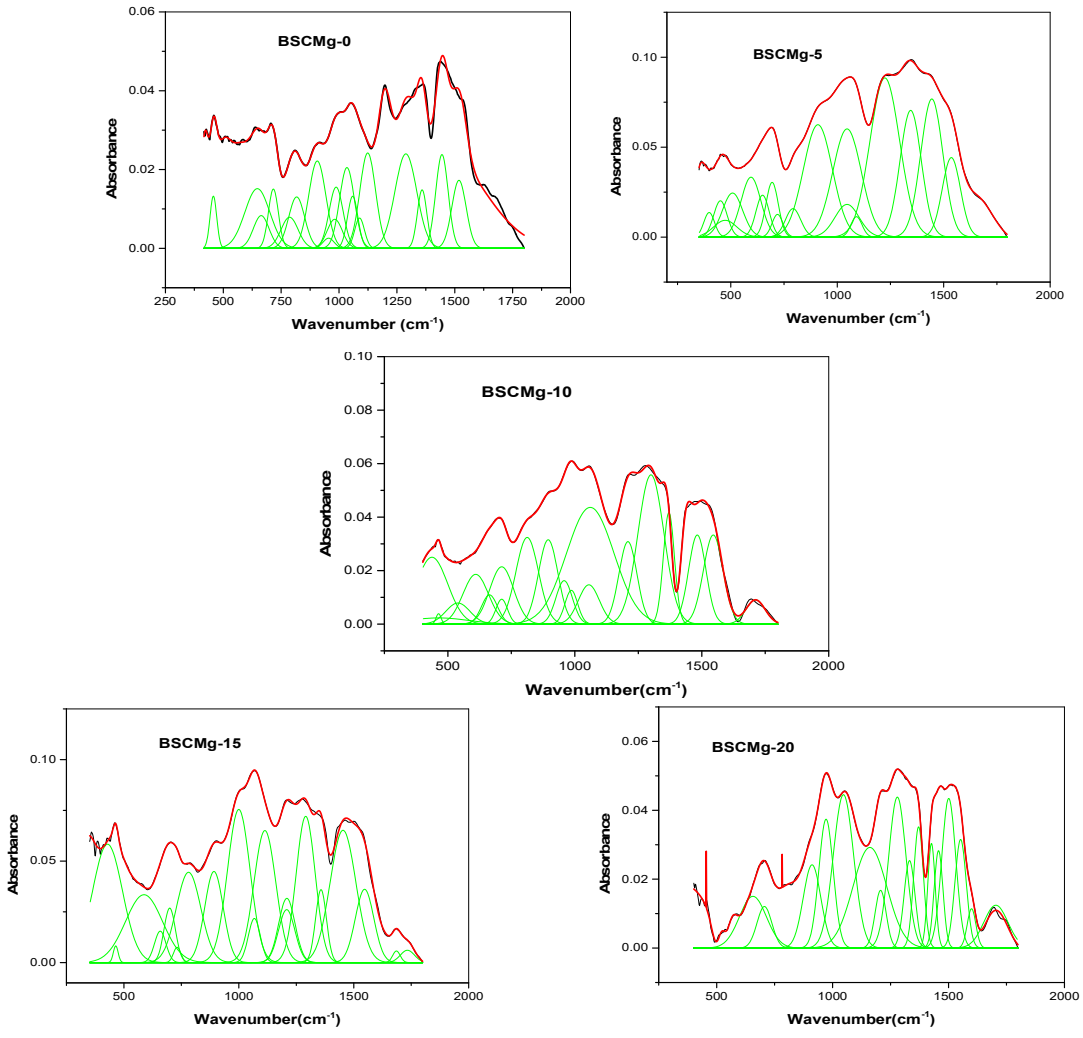

Fig.-8: (a-e) FTIR Fittings of (80-x) B_2O_3-10Sb_2O_3-10CaO-XMgO Where x = 0,5,10,15, and 20 mol%

Table-2: FTIR Band Positions of (80-x)B_2O_3-10Sb_2O_3-10CaO-XMgO Where x = 0,5,10,15, and 20 mol%

Characteristic bands	Assignment
395-418 cm^{-1}	Vibrations of MgO tetrahedral.
465-472 cm^{-1}	Bending vibrations of Ca-O structural units
695-700 cm^{-1}	Stretching vibrations of Sb-O-Sb in Sb-O linkage
793-812 cm^{-1}	Bending vibrations of B–O–B in BO_4 units
1219-1225 cm^{-1}	Stretching vibrations of B–O in BO_3 units from different borate groups.
2900-2981 cm^{-1}	H–O–H groups.

CONCLUSION

- The XRD spectra of all the studied glasses revealed the short-range order and lack of periodicity with the existence of broad humps near Braggs angle 28^0.
- The Archimedes principle-based density of MgO-incorporated borate glasses was shown increasing trends. The molar volumes decreased and it showed the opposite trend when compared to the density.
- The optical spectra data used in the calculations of cut-off, refractive index, Urbach, indirect, and direct band gap energies.
- The increasing trends were found in the cut-off edge, Urbach, and Refractive index.
- The decreasing trends were found in the indirect band gap and direct band gap.
- The stability of the present glasses proved with the higher refractive index of 2.3.
- The higher values of refractive index make the glasses prominent in optoelectronic device applications.

ACKNOWLEDGMENTS

The authors must be thankful to the Head of the Department of Chemistry, for the experimental facilities during the research work.

CONFLICT OF INTERESTS

The authors declare that there is no conflict of interest.

AUTHOR CONTRIBUTIONS

All the authors contributed significantly to this manuscript, participated in reviewing/editing, and approved the final draft for publication. The research profile of the authors can be verified from their ORCID IDs, given below:

A. Rajesh http://orchid.org/0009-0001-2111-3894
Pallati Naresh http://orchid.org/0000-0003-3663-5940
Jagram Anterbedy http://orchid.org/0009-0007-5819-0002
K. Santosh Kumari http://orchid.org/0000-0002-2576-5742
Gangadhar Thalari http://orchid.org/0000-0002-5037-2609

REFERENCES

1. M.I. Sayyed, K.A. Mahmoud, Kawa M. Kaky, *Annals of Nuclear Energy*, **208**, 110765(2024), https://doi.org/10.1016/j.anucene.2024.110765
2. Pallati Naresh, *Journal of Molecular Structure*, **1213**, 128184 (2020) https://doi.org/10.1016/j.molstruc.2020.128184
3. Ramesh Sopinti , Nagarjuna Gunnam , Bejjipurapu Chandrasekhar , Rajeswara Rao Darsi , G. Bhanu Kiran and Raghavaiah B.V, *Rasayan Journal of Chemistry*, **17(1)**, 47(2024), http://doi.org/10.31788/RJC.2024.1718549
4. G. Jebadoss Thinakaran, R. Sugaraj Samuel, M. Ajith Kumar and J. Prince Joshua, *Rasayan Journal of Chemistry*, **17(1)**, 172 (2024), http://doi.org/10.31788/RJC.2024.1718673
5. J.S. Ashwajeet, T. Sankarappa, T. Sujatha, R. Ramanna, *Journal of Non-Crystalline Solids*, **486**, 52 (2018), https://doi.org/10.1016/j.jallcom.2017.10.271
6. Al-Buriahi, M.S., Rashad, M., Alalawi, A.,Sayyed, M.I., *Ceramics International,* **46**, 16452 (2020), https://doi.org/10.1016/j.ceramint.2020.03.208
7. Bala, M., Agrohiya, S., Dahiya, S., Ohlan, A., Punia, R., Maan, A.S, *Journal of Molecular Struct*ure, **1219**, 128589 (2020), https://doi.org/10.1007/s12633-023-02832-6
8. Pallati Naresh, N. Narsimlu, Ch. Srinivas, Md. Shareefuddin, K. Siva Kumar *Journal of Non-Crystalline Solids,***549**, 120361(2020), https://doi.org/10.1016/j.jnoncrysol.2020.120361

9. M. Rajesh, M.R. Babu, N.J. Sushma, B.D.P. Raju, *Journal of Non-Crystalline Solids*, **528**, 119732(2020), https://doi.org/10.1016/j.jnoncrysol.2019.119732
10. Jamila S. Alzahrani, Andrei V. Lebedev, Samvel A. Avanesov, Alaa Hammoud, Z.A. Alrowaili, Zakaria M.M. Mahmoud, I.O. Olarinoye, M.S. Al-Buriahi, *Ceramics International*, **48(13)**,18330(2022), https://doi.org/10.1016/j.ceramint.2022.03.092
11. Sowmya Mudunuru, Ganapavarapu Veera Raghava Sharma, Chandra Sekhara Rao Gurubilli, Srinivasa Rao G. and Gowri Sankara Rao B., *Rasayan Journal of Chemistry*, **17(3)**, 838(2024), http://doi.org/10.31788/RJC.2024.1738868
12. Vinoda Rani M., Naresh Pallati, Ravi Kumar Vuradi, Sadananda Chary A., Narender Reddy S., *Journal of Non-Crystalline Solids*, **629**, 122862(2024), https://doi.org/10.1016/j.jnoncrysol.2024.122862
13. G. Sangeetha, K. Chandra Sekhar, M. Narasimha Chary, M. Shareefuddin, *Optik,* **259**, 168952 (2022), https://doi.org/10.1016/J.IJLEO.2022.168952
14. M. H. A. Mhareb, S. Hashim, S.K. Ghoshal, Y.S.M. Alajerami, M.A. Saleh, R.S. Dawaud, N.A.B. Razak, S. A. B. Azizan, *Optical Materials*, **37**, 391(2014), https://doi.org/10.1016/J.OPTMAT.2014.06.033
15. A. Ichoja, S. Hashim, S.K. Ghoshal, I.H. Hashim, R.S. Omar, *Journal of Rare Earths,* **36**,1264(2018), https://doi.org/10.1016/J.JRE.2018.05.013.
16. H. Doweidar, Y. BSaddeek, *Journal of Non-Crystalline Solids,* **355**, 348(2009), https://doi.org/10.1016/J.JNONCRYSOL.2008.12.008
17. M.S. Gaafar, N.S.A. El-Aal, O.W. Gerges, G. El-Amir, *Journal of Alloys and Compounds,* **475**, 535(2009), https://doi.org/10.1016/J.JALLCOM.2008.07.114
18. A.A. Ali, Y.S. Rammah, R. El-Mallawany, D. Souri, *Measurement,* **105**, 72(2017), https://doi.org/10.1016/J.MEASUREMENT.2017.04.010
19. E.Mansour, *Journal of Molecular Structure,* **1014**, 1(2012), https://doi.org/10.1016/J.MOLSTRUC.2012.01.034
20. P. Pascuta, R. Lungu, I. Ardelean, *Journal of Material Science: Materials in Electronics,* **21**, 548(2010), https://doi.org/10.1007/s10854-009-9955-7
21. A. Samir, M.A. Hassan, A. Abokhadra, L.I. Soliman, M. Elokr, *Optics and Quantum Electronics,* **51**, 123 (2019), https://doi.org/10.1007/s11082-019-1819-7
22. H. Al-Ghamdi, N.A.M. Alsaif, Z.Y. Khattari, R.A. Elsad, A.M. El-Refaey, M.S. Sadeq, Y.S. Rammah, M.A. El-Shorbagy, M.S. Shams, *Journal of Material Science: Materials in Electronics,* **34**, 1180 (2023) , https://doi.org/10.1007/s10854-023-10560-1
23. M. Tijaria, Y. Sharma, V. Kumar, S. Dahiya, J. Dalal, *Materials Today Proceedings,* **45**, 3722(2021), https://doi.org/10.1016/J.MATPR.2020.12.688
24. A. Saidu, H. Wagiran, M.A. Saeed, Y.S.M. Alajerami, *Optics and Spectroscopy,* **117**, 396(2014), https://doi.org/10.1134/S0030400X14090239
25. A.A. Abul-Magd, H.Y. Morshidy, A.M. Abdel-Ghany, *Optical Materials*, **109**,110301(2020), https://doi.org/10.1016/J.OPTMAT.2020.110301

[RJC- 8863/2024]